Noname manuscript No.
(will be inserted by the editor)

On the parameter choice in grad-div stabilization for the Stokes equations

Eleanor W. Jenkins · Volker John · Alexander Linke · Leo G. Rebholz

Abstract Standard error analysis for grad-div stabilization of inf-sup stable conforming pairs of finite element spaces predicts that the stabilization parameter should be optimally chosen to be $\mathcal{O}(1)$. This paper revisits this choice for the Stokes equations on the basis of minimizing the $H^1(\Omega)$ error of the velocity and the $L^2(\Omega)$ error of the pressure. It turns out, by applying a refined error analysis, that the optimal parameter choice is more subtle than known so far in the literature. It depends on the used norm, the solution, the family of finite element spaces, and the type of mesh. In particular, the approximation property of the pointwise divergence-free subspace plays a key role. With such an optimal approximation property and with an appropriate choice of the stabilization parameter, estimates for the $H^1(\Omega)$ error of the velocity are obtained that do not directly depend on the viscosity and the pressure. The minimization of the $L^2(\Omega)$ error of the pressure requires in many cases smaller stabilization parameters than the minimization of the $H^1(\Omega)$ velocity error. Altogether, depending on the situation, the optimal stabilization parameter could range from being very small to very large. The analytic results are supported by numerical examples. Applying the analysis to the MINI element leads to proposals for the stabilization parameter which seem to be new.

Keywords Incompressible Stokes equations · Mixed finite elements · Grad-div stabilization · Error estimates · Pointwise divergence-free subspace

Mathematics Subject Classification (2010) 65N30 · 76M10

1 Introduction

This paper investigates the choice of the parameter for grad-div stabilization in mixed finite element methods for the Stokes equations, which are given by

$$-\nu\Delta\mathbf{u} + \nabla p = \mathbf{f}, \quad \nabla\cdot\mathbf{u} = 0 \quad \text{in } \Omega.$$

Grad-div stabilization results from adding $\mathbf{0} = -\gamma\nabla(\nabla\cdot\mathbf{u})$ to the continuous Stokes equations, which yields the term $\gamma(\nabla\cdot\mathbf{u}_h, \nabla\cdot\mathbf{v}_h)$ in the finite element formulation. Since $\nabla\cdot\mathbf{u}_h \neq 0$ for most common finite element methods for the Stokes equations, due to the only discrete enforcement of the divergence-free condition, this

A. Linke supported by the DFG Research Center Matheon, project D27.

L. G. Rebholz partially supported by NSF grant DMS1112593.

E. W. Jenkins
Department of Mathematical Sciences, Clemson University, U.S.A., E-mail: lea@clemson.edu

V. John
Weierstrass Institute for Applied Analysis and Stochastics, Mohrenstr. 39, 10117 Berlin, Germany and Free University of Berlin, Department of Mathematics and Computer Science, Arnimallee 6, 14195 Berlin, Germany,
E-mail: volker.john@wias-berlin.de

A. Linke
Free University of Berlin, Department of Mathematics and Computer Science, Arnimallee 6, 14195 Berlin, Germany,
E-mail: alexander.linke@wias-berlin.de

L. G. Rebholz
Department of Mathematical Sciences, Clemson University, U.S.A., E-mail: rebholz@clemson.edu

additional term is non-zero and it acts to penalize a lack of mass conservation. This consistent stabilization term was first introduced in [8], and it is well known that its use can improve solution accuracy for Stokes [25] and Navier–Stokes equations [23,18], conditioning of discrete systems [13], convergence of iterative solvers [5,14], and even solution accuracy for related problems such as the Boussinesq equations and others [7,22,11,30,15].

Due to the proven usefulness of grad-div stabilization, there is a natural interest to deepen its understanding, and in particular to study how to choose the stabilization parameter γ optimally. Theoretical analysis (which considers the dependence of γ on the mesh width and the viscosity) and numerical simulations, originally performed in [28], and subsequently in [24,20,25,3,12], suggest that $\gamma = \mathcal{O}(1)$ is an appropriate choice in the context of inf-sup stable conforming finite element spaces, and this choice seems to be widely accepted in the community. However, it was recently shown in [11] that in certain situations, an optimal γ can actually be much larger than $\mathcal{O}(1)$. There, the authors showed analytically and with numerical studies that for solutions with large or complicated pressures, e.g., caused by irrotational forcing, one gets very good results with $\gamma = 10^4$ and bad results with $\gamma = 1$ or 10.

The goals of the present paper are to show for the simplest model problem, the Stokes equations, that

- the choice of the grad-div stabilization parameter from the analytic point of view is more involved than it can be found so far in the literature, if the error in the $H^1(\Omega)$ norm of the velocity is of primary interest,
- an enormous increase in accuracy can be achieved sometimes by using a parameter that is predicted by the analysis presented in this paper, instead of a standard $\mathcal{O}(1)$ parameter.

The Stokes equations are considered, e.g., instead of the Navier–Stokes equations, in order to concentrate on the main statement of this paper, the more subtle choice of the stabilization parameter than it is known so far, without introducing technical difficulties that arise, e.g., from the consideration of nonlinear problems. In particular, it will be shown first that for minimizing the $H^1(\Omega)$ velocity error the optimal parameter choice depends critically on the magnitude of the pressure relative to the velocity in appropriate norms. A statement of this form can be also found in [24,14], but the possibly large stabilization parameter is not investigated further. Secondly, it depends on whether the pointwise divergence-free subspace of the finite element velocity space has some optimal approximation properties, which seems to be a new observation. These properties are closely related with the specific choice of the finite element space, i.e., with the family of finite elements and with the mesh. The results will be derived by performing a finite element error analysis for the $H^1(\Omega)$ velocity error, considering it as a function of γ, and then minimizing it. Inserting the proposed parameter into the error estimate reveals that there will be no direct dependence of the bound on ν if a pointwise divergence-free subspace with optimal approximation property exists. It will be also shown that one obtains different optimal stabilization parameters if one considers the $L^2(\Omega)$ error of the pressure. These parameters are smaller in many cases than those obtained for the minimization of the $H^1(\Omega)$ velocity error, in particular if the viscosity is small.

It turns out, depending on the specific situation, that the optimal stabilization parameter might be of very different size, e.g., it depends on the norms of the velocity and pressure and the element choice, and might depend on the mesh width h, and the viscosity ν. For the MINI element, for example, the optimal γ decreases with h, but this is not true for the Taylor–Hood element. The proposed stabilization parameters for the MINI element seem to be new. We like to remark that although the theory consists essentially in refining a standard analysis, it is able to predict phenomena seemingly unobserved before. However, it does not lead to formulas for choosing the grad-div stabilization parameter that can be used instantly in practice since the formulas involve usually unknown constants and norms of derivatives of the velocity and pressure solution of the continuous Stokes equations. Instead, the theory provides a qualitative understanding for the practitioner, how the discretization method and the mesh influence the choice of a good stabilization parameter.

The paper starts by introducing the continuous and the discrete Stokes equations as well as the space of divergence-free and discretely divergence-free functions in Section 2. Section 3 presents the finite element error analysis that leads to good parameter choices for minimizing different errors and for different approximation properties of the pointwise divergence-free subspace. Numerical studies, presented in Section 4, support the analytic results. In particular, it is shown that, depending on the example, the finite element space, and the mesh, the optimal parameter might be vary from $\mathcal{O}(h^2)$ to $\mathcal{O}(10^4)$. Section 5 summarizes the results and further steps are discussed that are necessary for the application of the theory to more difficult problems than considered in this paper. Throughout the paper, we use the notation $(\cdot,\cdot)$ to represent the $L^2(\Omega)$ inner product, $\|\cdot\|_0$ the $L^2(\Omega)$ norm, and $|\cdot|_n$ the semi norm in $H^n(\Omega)$.

2 The setup of the problem and its finite element discretization

This paper considers the Stokes equations with homogeneous Dirichlet boundary conditions: find $(\mathbf{u}, p) \in H_0^1(\Omega)^d \times L_0^2(\Omega)$ in a Lipschitz domain with polyhedral boundary $\Omega \subset \mathbb{R}^d$, $d \in \{2, 3\}$, such that, for all $(\mathbf{v}, q) \in H_0^1(\Omega)^d \times L_0^2(\Omega)$ it holds

$$\begin{aligned} \nu(\nabla \mathbf{u}, \nabla \mathbf{v}) - (\nabla \cdot \mathbf{v}, p) &= (\mathbf{f}, \mathbf{v}), \\ (\nabla \cdot \mathbf{u}, q) &= 0. \end{aligned} \tag{2.1}$$

For the finite element discretization, we choose pairs of conforming finite element spaces $V_h \subset H_0^1(\Omega)^d$ and $Q_h \subset L_0^2(\Omega)$ that satisfy the inf-sup stability condition (BB condition, LBB condition), see, e.g. [4,17],

$$\inf_{q_h \in Q_h} \sup_{\mathbf{v}_h \in V_h} \frac{(\nabla \cdot \mathbf{v}_h, q_h)}{\|\nabla \mathbf{v}_h\|_0 \, \|q_h\|_0} \geq \beta > 0. \tag{2.2}$$

In addition, the discrete bilinear form is extended with a grad-div stabilization in order to mitigate problems with poor mass conservation. Then, the stabilized finite element discretization reads: For fixed $\gamma \geq 0$, find $(\mathbf{u}_h, p_h) \in V_h \times Q_h$ such that for all $(\mathbf{v}_h, q_h) \in V_h \times Q_h$

$$\begin{aligned} \nu(\nabla \mathbf{u}_h, \nabla \mathbf{v}_h) + \gamma(\nabla \cdot \mathbf{u}_h, \nabla \cdot \mathbf{v}_h) - (\nabla \cdot \mathbf{v}_h, p_h) &= (\mathbf{f}, \mathbf{v}_h), \\ (\nabla \cdot \mathbf{u}_h, q_h) &= 0. \end{aligned} \tag{2.3}$$

We introduce now the spaces of weakly differentiable pointwise divergence-free functions and discretely divergence-free functions, respectively,

$$\begin{aligned} V_0 &= \{\mathbf{v} \in H_0^1(\Omega)^d \ : \ \nabla \cdot \mathbf{v} = 0\}, \\ V_{0,h} &= \{\mathbf{v}_h \in V_h \ : \ (\nabla \cdot \mathbf{v}_h, q_h) = 0 \ \text{ for all } q_h \in Q_h\}. \end{aligned}$$

In general, $V_{0,h} \not\subset V_0$, i.e., discretely divergence-free functions need not to be pointwise divergence-free. Note that there are only few pairs of finite element spaces that satisfy $V_{0,h} \subset V_0$. The space of divergence-free and discretely divergence-free functions

$$V_{00,h} := V_{0,h} \cap V_0$$

will become important for an appropriate choice of the stabilization parameter γ.

Definition 1 (Optimal approximation properties of the divergence-free subspace) Consider a sequence of quasi-uniform meshes with characteristic mesh size h and the corresponding spaces $V_{00,h}$. If for all $\mathbf{v} \in V_0 \cap H^{k+1}(\Omega)^d$ there exists a sequence of $\mathbf{v}_h \in V_{00,h}$ with

$$\|\nabla \mathbf{v} - \nabla \mathbf{v}_h\|_0 \leq C_{V_{00,h}} h^k |\mathbf{v}|_{k+1},$$

with $C_{V_{00,h}}$ independent of h, then the sequence of spaces $V_{00,h}$ is said to possess optimal approximation properties (w.r.t. the space V_0).

There are several known combinations of element choices and mesh types where optimal approximation properties are known to hold for $V_{00,h}$, e.g. $X_h = (P_k)^d$ with $k \geq d$ on barycenter-refined triangular/tetrahedral meshes [27,2,31], and $X_h = (P_1)^2$ on Powell–Sabin grids [32] or Union Jack grids [33].

3 On choices of the grad-div parameter that are based on error estimates

The goal of the following analysis consists in finding good values for the stabilization parameter γ. It will be shown that the standard parameter choice $\gamma \sim \mathcal{O}(1)$, presented, e.g., in [25,29], is not always adequate, and that it can even be far from optimal. This standard choice is justified in a paradigmatic way in the excellent article [25] by deriving an optimal a-priori estimate for (2.3). We like to emphasize that the discussion of an appropriate stabilization parameter in [25] is based on the norm $(\nu^{\frac{1}{2}} \|\nabla \mathbf{u}\|_0 + \gamma^{\frac{1}{2}} \|\nabla \cdot \mathbf{u}\|_0 + \|p\|_0)$. The choice of an optimal γ is not really investigated there. Rather more, it is argued that the choice $\gamma = \mathcal{O}(1)$ leads to a discrete problem that is uniformly well-posed in the corresponding energy norm with respect to ν. Similarly, in [24] an optimal error estimate is derived in the norm $(\nu \|\nabla \mathbf{u}\|_0^2 + \gamma \|\nabla \cdot \mathbf{u}\|_0^2 + \|p\|_0^2)^{\frac{1}{2}}$, and an optimal γ is derived from the right hand side of the estimate.

In contrast, this paper studies first the optimality with respect to the velocity norm $\|\nabla \mathbf{u}\|_0$ alone, since one is often mainly interested in the control of this error. Such an estimate also allows to track the influence of the divergence error in a more appropriate way, and it will be revealed that the existence of a divergence-free subspace with optimal approximation properties changes the optimal choice of the grad-div stabilization parameter significantly. Moreover, problems are avoided that arise from including γ into the error norm on the left hand side of the error estimate and simultaneously varying γ in the right side of the error estimate. Note that for large γ on a fixed grid the term $\gamma^{\frac{1}{2}} \|\nabla \cdot \mathbf{u}\|_0$ goes to zero only with $\mathcal{O}(\gamma^{-\frac{1}{2}})$ [19]. Following this analysis, it will be verified that the asymptotic optimal choice of γ which is based on the consideration of the error in the $L^2(\Omega)$ pressure norm leads to different values as were derived for the error in the velocity norm. The choice of a different norm with respect to the derivations in [25,29], as well as the refined analysis, seem to explain the different results.

3.1 Appropriate choices of the grad-div parameter based on a velocity error estimate

We consider now the $H^1(\Omega)$ velocity error of the discrete Stokes system with grad-div stabilization (2.3) and use the resulting error estimate to find a good choice for γ.

Theorem 1 *For a given $\mathbf{f} \in H^{-1}(\Omega)^d$, let $(\mathbf{u}, p)$ be the solution to (2.1), and let $(\mathbf{u}_h, p_h)$ be the solution to (2.3). Then, the error in the $L^2(\Omega)$ norm of the gradient of the velocity is bounded by*

$$\|\nabla(\mathbf{u}-\mathbf{u}_h)\|_0^2 \leq \inf_{\mathbf{w}_h \in V_{0,h}} \left(4\|\nabla(\mathbf{u}-\mathbf{w}_h)\|_0^2 + 2\frac{\gamma}{\nu}\|\nabla\cdot\mathbf{w}_h\|_0^2\right) + \frac{2}{\gamma\nu}\inf_{q_h\in Q_h}\|p-q_h\|_0^2. \tag{3.1}$$

Proof Write $\mathbf{u}-\mathbf{u}_h = (\mathbf{u}-\mathbf{w}_h) + (\mathbf{w}_h - \mathbf{u}_h) =: \boldsymbol{\eta} + \boldsymbol{\psi}_h$, where $\mathbf{w}_h \in V_{0,h}$ is arbitrary. First, by the triangle inequality and Young's inequality, one obtains

$$\|\nabla\mathbf{u} - \nabla\mathbf{u}_h\|_0^2 \leq 2\,\|\nabla\boldsymbol{\eta}\|_0^2 + 2\,\|\nabla\boldsymbol{\psi}_h\|_0^2\,. \tag{3.2}$$

For any $\mathbf{v}_h \in V_{0,h}$, one concludes by subtracting (2.1) and (2.3) that

$$\nu(\nabla\boldsymbol{\psi}_h, \nabla\mathbf{v}_h) + \gamma(\nabla\cdot\boldsymbol{\psi}_h, \nabla\cdot\mathbf{v}_h) = -\nu(\nabla\boldsymbol{\eta}, \nabla\mathbf{v}_h) - \gamma(\nabla\cdot\boldsymbol{\eta}, \nabla\cdot\mathbf{v}_h) + (\nabla\cdot\mathbf{v}_h, p).$$

Choosing $\mathbf{v}_h = \boldsymbol{\psi}_h$, and using that $(\nabla\cdot\boldsymbol{\psi}_h, q_h) = 0$ for any $q_h \in Q_h$, the error equation becomes, for any $q_h \in Q_h$,

$$\nu\|\nabla\boldsymbol{\psi}_h\|_0^2 + \gamma\|\nabla\cdot\boldsymbol{\psi}_h\|_0^2 = -\nu(\nabla\boldsymbol{\eta}, \nabla\boldsymbol{\psi}_h) - \gamma(\nabla\cdot\boldsymbol{\eta}, \nabla\cdot\boldsymbol{\psi}_h) + (\nabla\cdot\boldsymbol{\psi}_h, p - q_h).$$

After applying the Cauchy-Schwarz and Young's inequality on the right hand side, one gets

$$\nu\|\nabla\boldsymbol{\psi}_h\|_0^2 + \gamma\|\nabla\cdot\boldsymbol{\psi}_h\|_0^2 \leq \nu\|\nabla\boldsymbol{\eta}\|_0^2 + \gamma\|\nabla\cdot\boldsymbol{\eta}\|_0^2 + 2\|p-q_h\|_0\|\nabla\cdot\boldsymbol{\psi}_h\|_0. \tag{3.3}$$

The last term on the right hand side can be estimated by

$$2\|p-q_h\|_0\|\nabla\cdot\boldsymbol{\psi}_h\|_0 \leq \gamma^{-1}\|p-q_h\|_0^2 + \gamma\|\nabla\cdot\boldsymbol{\psi}_h\|_0^2, \tag{3.4}$$

which leads to

$$\|\nabla\boldsymbol{\psi}_h\|_0^2 \leq \|\nabla\boldsymbol{\eta}\|_0^2 + \frac{\gamma}{\nu}\|\nabla\cdot\boldsymbol{\eta}\|_0^2 + \frac{1}{\gamma\nu}\inf_{q_h\in Q_h}\|p-q_h\|_0^2.$$

Finally, (3.2) gives

$$\|\nabla\mathbf{u} - \nabla\mathbf{u}_h\|_0^2 \leq 4\|\nabla\boldsymbol{\eta}\|_0^2 + 2\frac{\gamma}{\nu}\|\nabla\cdot\boldsymbol{\eta}\|_0^2 + \frac{2}{\gamma\nu}\inf_{q_h\in Q_h}\|p-q_h\|_0^2$$

for all $\mathbf{w}_h \in V_{0,h}$, which is just the statement of the theorem. ■

The key of the analysis consists in tracking the divergence error to the final estimate (3.1). This estimate allows to study the consequences of the error bound (3.1) on the choice of γ for two different cases. These two cases are characterized by whether or not the pointwise divergence-free subspace of the velocity space has optimal approximation properties.

Corollary 1 (Taylor–Hood elements) *Consider* $(V_h, Q_h) = ((P_k)^d, P_{k-1})$ *on quasi-uniform meshes and assume that the solution* $(\mathbf{u}, p)$ *of* (2.1) *lies in* $H^{k+1}(\Omega)^d \times H^k(\Omega)$.

Case 1) In the general case, if $V_{00,h}$ *does not have optimal approximation properties, then the a-priori estimate of Theorem 1 has the form*

$$\|\nabla \mathbf{u} - \nabla \mathbf{u}_h\|_0^2 \leq \left(4 + \frac{2\gamma}{\nu}\right) C_{V_{0,h}}^2 h^{2k} |\mathbf{u}|_{k+1}^2 + \frac{2C_{Q_h}^2}{\gamma\nu} h^{2k} |p|_k^2. \tag{3.5}$$

Case 2) If $V_{00,h}$ *has optimal approximation properties, one obtains the a-priori error estimate*

$$\|\nabla \mathbf{u} - \nabla \mathbf{u}_h\|_0^2 \leq \min\left\{\left(4 + \frac{2\gamma}{\nu}\right) C_{V_{0,h}}^2, 4C_{V_{00,h}}^2\right\} h^{2k} |\mathbf{u}|_{k+1}^2 + \frac{2C_{Q_h}^2}{\gamma\nu} h^{2k} |p|_k^2. \tag{3.6}$$

The constants $C_{Q_h}, C_{V_{00,h}}, C_{V_{0,h}}$ *are constants coming from interpolation estimates, where* $C_{V_{00,h}}$ *and* $C_{V_{0,h}}$ *depend on* β^{-1}.

Proof For the first case, one can only use that $\|\nabla \cdot \mathbf{w}_h\| = \|\nabla \cdot (\mathbf{u} - \mathbf{w}_h)\| \leq \|\nabla(\mathbf{u} - \mathbf{w}_h)\|$ holds in this setting. Then, one applies standard approximation theory to prove (3.5).

For the second case, if the space $V_{00,h}$ has optimal approximation properties, one gets an additional estimate. Here, one can choose $\mathbf{w}_h \in V_{00,h}$ in (3.1). Hence, the velocity error term can be bounded also by

$$\inf_{\mathbf{w}_h \in V_{0,h}} \left(4\|\nabla(\mathbf{u} - \mathbf{w}_h)\|_0^2 + 2\frac{\gamma}{\nu}\|\nabla \cdot \mathbf{w}_h\|_0^2\right) \leq 4C_{V_{00,h}}^2 h^{2k} |\mathbf{u}|_{k+1}^2,$$

since $2\frac{\gamma}{\nu}\|\nabla \cdot \mathbf{w}_h\|_0^2$ vanishes. Combining both results gives (3.6). Since $V_{00,h} \subset V_{0,h}$, one expects that $C_{V_{00,h}}$ is larger than $C_{V_{0,h}}$. ∎

Remark 1 (Taylor–Hood elements) The two different cases from Corollary 1 will be discussed now in more detail.

Case 1) If $V_{00,h}$ does not have optimal approximation properties, one can regard the right hand side of (3.5) as a function dependent on γ. This function has a minimum which can be determined by elementary calculus:

$$\gamma_{\text{opt}} \approx \frac{C_{Q_h}}{C_{V_{0,h}}} \frac{|p|_k}{|\mathbf{u}|_{k+1}}. \tag{3.7}$$

Hence, with respect to ν and h, the standard parameter choice $\gamma = \mathcal{O}(1)$ is recovered. However, we emphasize that γ_{opt} from (3.7) may be quite large, whenever the velocity norm is small compared with the pressure norm, and that this situation can happen in practice, e.g., in coupled flow problems like Rayleigh–Bénard convection, see Section 4. Moreover, inserting γ_{opt} into the error estimate (3.5) gives

$$\|\nabla \mathbf{u} - \nabla \mathbf{u}_h\|_0 \leq 2h^k \left(C_{V_{0,h}}^2 |\mathbf{u}|_{k+1}^2 + \frac{1}{\nu} C_{V_{0,h}} C_{Q_h} |\mathbf{u}|_{k+1} |p|_k\right)^{1/2}. \tag{3.8}$$

This error estimate reveals a direct dependence of the optimal velocity solution on $(|p|_k/\nu)^{1/2}$, even for the best possible stabilization parameter. In other words, even if the approximation space $V_{0,h}$ can approximate the velocity solution $\mathbf{u}$ perfectly, it is not guaranteed that the discrete (grad-div)-stabilized solution is a good approximation. The grad-div stabilization is therefore able to mitigate the problem of poor mass conservation, but in general not able to heal it perfectly.

Case 2) If $V_{00,h}$ has optimal approximation properties, the right hand side of estimate (3.6) is not as easy to analyze. The numerical results in Figure 2 show, depending on the complexity of the pressure, there may or there may be not an optimal γ, since for $|p|_k \gg |\mathbf{u}|_{k+1}$ one has $\gamma_{\text{opt}} = \infty$, which is not feasible in practice (but is equivalent to using $((P_2)^2, P_1^{\text{disc}})$ Scott–Vogelius elements [6]). Therefore, giving up the idea of finding the optimal γ, we only want to find a good γ, which should not be ∞. We used as criterion for the choice of γ that the contribution of the pressure error equals the maximum possible contribution of the velocity error $4C_{V_{00,h}}^2 h^{2k} |\mathbf{u}|_{k+1}^2$, which is already asymptotically optimal. This criterion leads to

$$\gamma_{\text{good}} \approx \frac{1}{2\nu} \left(\frac{C_{Q_h}}{C_{V_{00,h}}} \frac{|p|_k}{|\mathbf{u}|_{k+1}}\right)^2. \tag{3.9}$$

The numerical studies in Section 4 will show that this consideration delivers good results. It is interesting that only in the second case γ_{good} is ν-dependent, which can be observed in the numerical examples as well. In addition, inserting γ_{good} into (3.6) gives the error estimate

$$\|\nabla \mathbf{u} - \nabla \mathbf{u}_h\|_0 \leq \sqrt{8} C_{V_{00,h}} |\mathbf{u}|_{k+1} h^k, \tag{3.10}$$

which does not directly depend on ν and p, but of course $|\mathbf{u}|_{k+1}$ might still depend on ν. If $|\mathbf{u}|_{k+1}$ does not depend on ν, (3.10) shows that the grad-div stabilization is able to deliver optimal robust approximations, if there exists a subspace of optimally converging divergence-free trial functions.

For both cases, one does not observe a dependence on the mesh width h. The dependence of the stabilization parameter on higher order norms of the solution can be already found in [24,14].

The corollary and remark above are specific to Taylor–Hood elements, but the same techniques can be applied to any conforming inf-sup stable finite element pair used for computing solutions of (2.3). Naturally, results for optimal stabilization parameter γ will vary. In the numerical experiments in Section 4, the theory will be tested on both the Taylor–Hood element and the MINI element.

3.2 Appropriate choices of the grad-div parameter based on a pressure error estimate

We consider now the effect of grad-div stabilization on the $L^2(\Omega)$ pressure error and how the optimal parameter scales with the problem data.

Theorem 2 *For a given $\mathbf{f} \in H^{-1}(\Omega)^d$, let $(\mathbf{u}, p)$ be the solution to (2.1), let $(\mathbf{u}_h, p_h)$ be the solution to (2.3), and assume for the inf-sup constant $0 < \beta \leq \mathcal{O}(1)$. Then the pressure error is bounded by*

$$\begin{aligned}\|p - p_h\|_0 \leq C(\beta^{-1}) \Bigg\{ & \left(1 + \left(\frac{\nu}{\gamma}\right)^{1/2}\right) \inf_{q_h \in Q_h} \|p - q_h\|_0 \\ & + \inf_{\mathbf{w}_h \in V_{0,h}} \left(\left(\nu + (\nu\gamma)^{1/2}\right) \|\nabla(\mathbf{u} - \mathbf{w}_h)\|_0 + \left((\nu\gamma)^{1/2} + \gamma\right) \|\nabla \cdot \mathbf{w}_h\|_0 \right) \Bigg\}. \end{aligned} \tag{3.11}$$

Proof From Equations (2.1) and (2.3) it follows that $\forall \mathbf{v}_h \in V_h$

$$(p - p_h, \nabla \cdot \mathbf{v}_h) = \nu(\nabla(\mathbf{u} - \mathbf{u}_h), \nabla \mathbf{v}_h) + \gamma(\nabla \cdot (\mathbf{u} - \mathbf{u}_h), \nabla \cdot \mathbf{v}_h).$$

Writing $p - p_h = (p - q_h) + (q_h - p_h)$ for arbitrary $q_h \in Q_h$, and dividing both sides by $\|\nabla \mathbf{v}_h\|$ and reducing gives

$$\begin{aligned}\frac{(q_h - p_h, \nabla \cdot \mathbf{v}_h)}{\|\nabla \mathbf{v}_h\|_0} &= \nu \frac{(\nabla(\mathbf{u} - \mathbf{u}_h), \nabla \mathbf{v}_h)}{\|\nabla \mathbf{v}_h\|_0} + \gamma \frac{(\nabla \cdot (\mathbf{u} - \mathbf{u}_h), \nabla \cdot \mathbf{v}_h)}{\|\nabla \mathbf{v}_h\|_0} - \frac{(\nabla \cdot \mathbf{v}_h, p - q_h)}{\|\nabla \mathbf{v}_h\|_0} \\ &\leq \nu \|\nabla(\mathbf{u} - \mathbf{u}_h)\|_0 + \gamma \|\nabla \cdot (\mathbf{u} - \mathbf{u}_h)\|_0 + \|p - q_h\|_0 .\end{aligned}$$

Next, applying the inf-sup stability (2.2) implies that

$$\beta \|p_h - q_h\|_0 \leq \nu \|\nabla(\mathbf{u} - \mathbf{u}_h)\|_0 + \gamma \|\nabla \cdot (\mathbf{u} - \mathbf{u}_h)\|_0 + \|p - q_h\|_0$$

for any $q_h \in Q_h$. Hence by the triangle equality one obtains

$$\|p - p_h\|_0 \leq \frac{\nu}{\beta} \|\nabla(\mathbf{u} - \mathbf{u}_h)\|_0 + \frac{\gamma}{\beta} \|\nabla \cdot (\mathbf{u} - \mathbf{u}_h)\|_0 + \left(1 + \frac{1}{\beta}\right) \inf_{q_h \in Q_h} \|p - q_h\|_0 . \tag{3.12}$$

From (3.1) it follows immediately that

$$\|\nabla(\mathbf{u} - \mathbf{u}_h)\|_0 \leq \inf_{\mathbf{w}_h \in V_{0,h}} \left(2\|\nabla(\mathbf{u} - \mathbf{w}_h)\|_0 + \left(\frac{2\gamma}{\nu}\right)^{1/2} \|\nabla \cdot \mathbf{w}_h\|_0 \right) + \left(\frac{2}{\gamma\nu}\right)^{1/2} \inf_{q_h \in Q_h} \|p - q_h\|_0. \tag{3.13}$$

Applying to (3.3)

$$2\|p - q_h\|_0 \|\nabla \cdot \boldsymbol{\psi}_h\|_0 \leq 2\gamma^{-1} \|p - q_h\|_0^2 + \frac{\gamma}{2} \|\nabla \cdot \boldsymbol{\psi}_h\|_0^2$$

instead of (3.4), one can derive with the same arguments the estimate

$$\|\nabla\cdot(\mathbf{u}-\mathbf{u}_h)\|_0 \leq \inf_{\mathbf{w}_h\in V_{0,h}} \left(\left(\frac{2\nu}{\gamma}\right)^{1/2} \|\nabla(\mathbf{u}-\mathbf{w}_h)\|_0 + \left(1+\sqrt{2}\right)\|\nabla\cdot\mathbf{w}_h\|_0 \right) + \frac{2}{\gamma}\inf_{q_h\in Q_h}\|p-q_h\|_0. \quad (3.14)$$

Then from (3.12)–(3.14), one gets

$$\|p-p_h\|_0 \leq \beta^{-1}\Bigg\{ \left(\beta+1+2+\left(\frac{2\nu}{\gamma}\right)^{1/2}\right)\inf_{q_h\in Q_h}\|p-q_h\|_0 + \inf_{\mathbf{w}_h\in V_{0,h}} \left(\left(2\nu+(2\nu\gamma)^{1/2}\right)\|\nabla(\mathbf{u}-\mathbf{w}_h)\|_0 + \left((2\nu\gamma)^{1/2}+\left(1+\sqrt{2}\right)\gamma\right)\|\nabla\cdot\mathbf{w}_h\|_0 \right)\Bigg\},$$

and assuming that $\beta \leq \mathcal{O}(1)$ allows this to be reduced to (3.11). ■

Note that the assumption on β is without loss of generality. If (2.2) holds for some positive β, it holds also for all positive stabilization parameters smaller than β.

The impact of the error bound (3.11) on the choice of the stabilization parameter will be studied in more detail again for the pairs of Taylor–Hood elements.

Corollary 2 (Taylor–Hood elements) *Let the conditions of Corollary 1 hold.*

Case 1) If $V_{00,h}$ does not have optimal approximation properties, one obtains the error estimate

$$\|p-p_h\|_0 \leq C(\beta^{-1})\left(\left(1+\left(\frac{\nu}{\gamma}\right)^{1/2}\right)C_{Q_h}h^k|p|_k + \left(\nu+(\nu\gamma)^{1/2}+\gamma\right)C_{V_{0,h}}h^k|\mathbf{u}|_{k+1}\right). \quad (3.15)$$

Case 2) If $V_{00,h}$ has optimal approximation properties, the a-priori error estimate becomes

$$\|p-p_h\|_0 \leq C(\beta^{-1})\Bigg(\left(1+\left(\frac{\nu}{\gamma}\right)^{1/2}\right)C_{Q_h}h^k|p|_k + \min\left\{\left(\nu+(\nu\gamma)^{1/2}+\gamma\right)C_{V_{0,h}}, \left(\nu+(\nu\gamma)^{1/2}\right)C_{V_{00,h}}\right\}h^k|\mathbf{u}|_{k+1}\Bigg). \quad (3.16)$$

Proof The statements follow with the same arguments as were used in the proof of Corollary 1. ■

Remark 2 Similarly to the velocity case, we want to find good values for γ. However, minimizing the a priori error estimate with respect to γ is more complex than in the velocity case. For instance, the necessary condition for getting the optimal value of γ from (3.15) leads to an equation of the form

$$\frac{\nu}{4}\left(\frac{C_{Q_h}|p|_k}{C_{V_{0,h}}|\mathbf{u}|_{k+1}}-\gamma\right)^2 = \gamma^3. \quad (3.17)$$

Standard calculus gives that there is at least one non-negative value of γ that satisfies (3.17) which is smaller than $(C_{Q_h}|p|_k)/(C_{V_{0,h}}|\mathbf{u}|_{k+1})$. This value is the most left non-negative intersection of the curves on both sides of (3.17). Since the right hand side of (3.15) is a continuous function for $\gamma\in(0,\infty)$ with the limit ∞ at both ends of this interval, the most left local extremum must be a minimum. In the interesting case that ν is small, the curve on the left hand side of (3.17) becomes flat and then there will be exactly one intersection of both curves, which has to correspond to a minimum and which has to be smaller than $(C_{Q_h}|p|_k)/(C_{V_{0,h}}|\mathbf{u}|_{k+1})$. We could not obtain an analytic expression for this minimum, but a comparison with (3.7) shows already that one gets a different (smaller) optimum than obtained for minimizing the $H^1(\Omega)$ error of the velocity. In the case of small ν, where the lowest power of ν is of importance, a slight dependence $\gamma_{\text{good}} = \mathcal{O}(\nu^{1/3})$ can be deduced from (3.17).

Considering Case 2 on the same basis like in Remark 1 gives

$$\gamma_{\text{good}} = \frac{C_{Q_h}|p|_k}{C_{V_{00,h}}|\mathbf{u}|_{k+1}}. \quad (3.18)$$

Again, the parameter is different from those obtained for minimizing the $H^1(\Omega)$ error of the velocity. In contrast to (3.9), the parameter (3.18) does not depend on the inverse of ν such that one can expect that for small ν the parameter (3.9) is larger than (3.18).

4 Numerical experiments

Two numerical experiments will be presented in this section. The first one is for an analytic test problem with known solution to support the analysis. In this experiment, the optimal values for γ can be computed and these values will be compared with the predictions from Section 3. The second example is of more practical interest; it is a Rayleigh–Bénard convection for silicon oil. Here, an analytic expression for the analytic solution is unknown, but from experiments one can hypothesize that $|p|_2/|\mathbf{u}|_3$ is very large, and therefore large grad-div stabilization parameters may significantly improve results. It will be verified that this is indeed the case.

4.1 Optimal stabilization parameters for an analytic test problem

This section will verify that the different regimes for choosing γ_{opt} or γ_{good} given in the previous section can be observed in numerical simulations. Examples with prescribed analytic solutions will be considered. Further steps of the application of the analytic results to more complicated situations will be pointed out at the end of Section 4.1.

The discretization of the Stokes problem was studied with two choices of conforming inf-sup stable pairs of finite element spaces and with three types of meshes. We considered (2.1) with $\Omega = (0,1)^2$ and with the prescribed velocity solution

$$\mathbf{u} = \begin{pmatrix} \cos(2\pi y) \\ \sin(2\pi x) \end{pmatrix}.$$

Four values for the viscosity were studied, $\nu \in \{1, 10^{-1}, 10^{-3}, 10^{-6}\}$, and three different functions that serve as a prescribed pressure solution:

$$p_1 = \sin(2\pi y), \qquad p_2 = \sin(8\pi y), \qquad p_3 = 10^4 \sin(2\pi y).$$

For each of these solutions, the forcing $\mathbf{f}$ was computed using the Stokes equation. In all examples, Dirichlet boundary conditions for the velocity were applied. The discrete problem (2.3) was then solved with varying stabilization parameter $\gamma \in [10^{-3}, 10^4]$. More than 500 values for γ were chosen in this interval, with finer distances for small γ and increasing distances for large γ. The simulations were performed with the code MooNMD [16] and selected results were double checked with freeFEM [10].

The first purpose of the numerical studies was to verify that the analysis-based selections of γ_{opt} or γ_{good}, e.g., see (3.7) or (3.9) for the Taylor–Hood finite element, are close to the actual optimal γ, in the sense of minimizing the $H^1(\Omega)$ velocity error. Secondly, the optimal stabilization parameters were computed also on the basis of minimizing the $L^2(\Omega)$ error of the pressure to show the differences to the velocity case and to illustrate the predictions from Remark 2.

There are unknown interpolation constants in the predictions of the optimal stabilization parameter. For each simulation, after having found the optimal parameter, one can compute an estimate of these constants. To get some idea of the magnitude of these constants, for all results with respect to the velocity error in the $H^1(\Omega)$ norm, we computed the estimate if the optimal parameter was not a boundary point of the interval $[10^{-3}, 10^4]$. Then, the three smallest and the three largest of these estimates were neglected (to remove extreme values which might come from round-off errors, see below) and from the remaining estimates the median and the arithmetic mean will be given.

Delaunay triangulations, barycenter refinements of triangular meshes, and Union Jack (criss-cross) meshes were considered. The use of these meshes allows to study the cases of optimal vs. non-optimal approximation properties of the pointwise divergence-free subspaces of the velocity spaces for the $((P_2)^2, P_1)$ and the $((P_1^{\text{bub}})^2, P_1)$ pairs of finite elements. From [2,27] it is known that the pointwise divergence-free subspace of the $(P_2)^2$ velocity space has optimal approximation properties on a barycenter refinement of a regular mesh. Also, the pointwise divergence-free subspace of the $(P_1^{\text{bub}})^2$ velocity on Union Jack meshes has optimal approximation properties, see [33]. An example of each of the considered mesh types is shown in Figure 1.

From the available numerical analysis, which tracks the dependence of the stabilization parameter on the viscosity and the mesh width, the proposal for this parameter is $\gamma = \mathcal{O}(1)$ in the case of inf-sup stable pairs of finite element spaces of Taylor–Hood type, [3,21]. The analysis of Section 3 leads to the same asymptotics for the case that the divergence-free subspace does not possess the optimal approximation property, see (3.7). However, in the other case, the dependence $\mathcal{O}(\nu^{-1})$ is predicted, see (3.9).

We could not find in the literature studies of the grad-div stabilization for the MINI element. However, the use of the MINI element $((P_1^{\text{bub}})^2, P_1)$ for the Stokes problem is equivalent to applying the PSPG

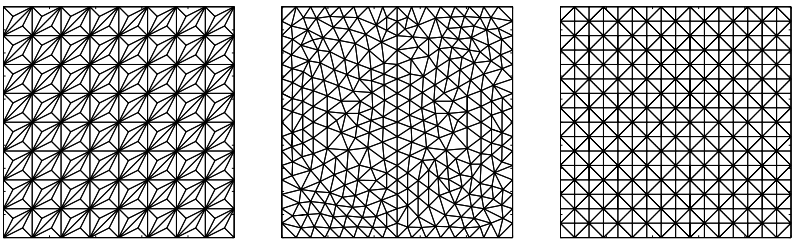

Fig. 1 Barycenter-refined ($h = 1/8$), Delaunay ($h = 1/16$), and Union Jack (criss-cross, $h = 1/16$) meshes (left to right) used in the numerical studies.

stabilization with the equal-order pair $((P_1)^2/P_1)$ with a special choice of the PSPG parameter [26]. The finite element error analysis of the PSPG/grad-div stabilization for the $((P_1)^2/P_1)$ pair of finite element spaces applied to the Stokes equations proposes to choose $\gamma = \mathcal{O}(\nu)$ [8,9,21,3]. In this analysis, contributions from the PSPG stabilization are used to estimate the coupled velocity-pressure terms of the weak form of the Stokes equations. In the analysis of Section 3, these terms had to be estimated in a different way. It will turn out that the application of the results of Section 3 to the MINI element lead to different proposals for γ than $\mathcal{O}(\nu)$, namely $\mathcal{O}(h^2/\nu)$ or $\mathcal{O}(h)$, depending on the approximation property of the pointwise divergence-free subspace. Since the results from Sections 4.1.3 and 4.1.4 indicate that $\gamma = \mathcal{O}(\nu)$ is often a bad choice for small ν, we do not wish to call it the standard choice for the grad-div parameter. Altogether, we could not identify a parameter choice which is standard for the MINI element.

To unify and simplify the presentation of the numerical results, the analytically proposed parameters will be denoted by γ_{good} below and the "optimal γ" will be the stabilization parameter that corresponds to the actually best results in the simulations.

4.1.1 $((P_2)^2, P_1)$ *Taylor–Hood element on barycenter-refined meshes*

First, the $((P_2)^2, P_1)$ Taylor–Hood element on a barycenter-refined uniform mesh is considered, a case where it is known that the divergence-free subspace of the velocity space has optimal approximation properties [2]. Thus, following the scaling analysis of the previous section, a good choice of γ for this test problem for minimizing the $H^1(\Omega)$ velocity error will satisfy, see (3.9),

$$\gamma_{\text{good}} \approx C_0 \frac{1}{2\nu} \frac{|p|_2^2}{|\mathbf{u}|_3^2} = \begin{cases} \dfrac{C_0}{16\nu\pi^2} & \text{for } p_1, \\ \dfrac{16C_0}{\nu\pi^2} & \text{for } p_2, \\ \dfrac{10^8 C_0}{16\nu\pi^2} & \text{for } p_3, \end{cases} \tag{4.1}$$

where C_0 is an unknown constant, which is independent of h and γ. Numerical simulations were performed on three meshes, with $h \in \{1/8, 1/16, 1/32\}$ (the $h = 1/8$ mesh is shown in Figure 1 on the left hand side).

The results of the numerical studies are presented in Figure 2, where the $H^1(\Omega)$ velocity error is plotted against the grad-div stabilization parameter γ. The legends contain the actual optimal values of γ and the $H^1(\Omega)$ velocity error for the standard choice $\gamma = 1$ (std.). The qualitative behavior of the results in relation with the predictions from (4.1) will be discussed. From (4.1) one expects an increase of the optimal parameter for decreasing viscosities. A good situation for observing this behavior are the cases where $|p|_2^2/|\mathbf{u}|_3^2$ is small, i.e., the cases p_1 and p_2. In Figure 2, one can see the expected behavior always for p_1 (first column) and mostly for p_2 (second column). For the case p_2 it should be noted that the error is always almost constant for all viscosities and $\gamma \gtrsim 100$. In such a situation, small changes of the velocity errors due to round-off errors might become important for the determination of the optimal stabilization parameter. Next, one expects from (4.1) that γ increases notably if $|p|_2^2$ increases. This effect is clearly visible by comparing, on the one hand, p_2 and p_1 (second and first column) and, on the other hand, p_3 and p_2 (third and second column). The next prediction is that very large optimal γ occur if ν is very small or $|p|_2^2$ is large. Finally, one does not expect a dependence of the optimal γ on the mesh width. Both expectations were always met. For C_0 in (4.1), the mean value 3.36 and the median 3.33 were estimated.

With respect to the accuracy of the computed solution, one can see clearly that in the case of $|p|_2^2$ being large, i.e. for p_3 (third column), the errors computed with the optimal γ are smaller by several orders of magnitude than the errors obtained with the standard parameter $\gamma = 1$. The independence of the error for

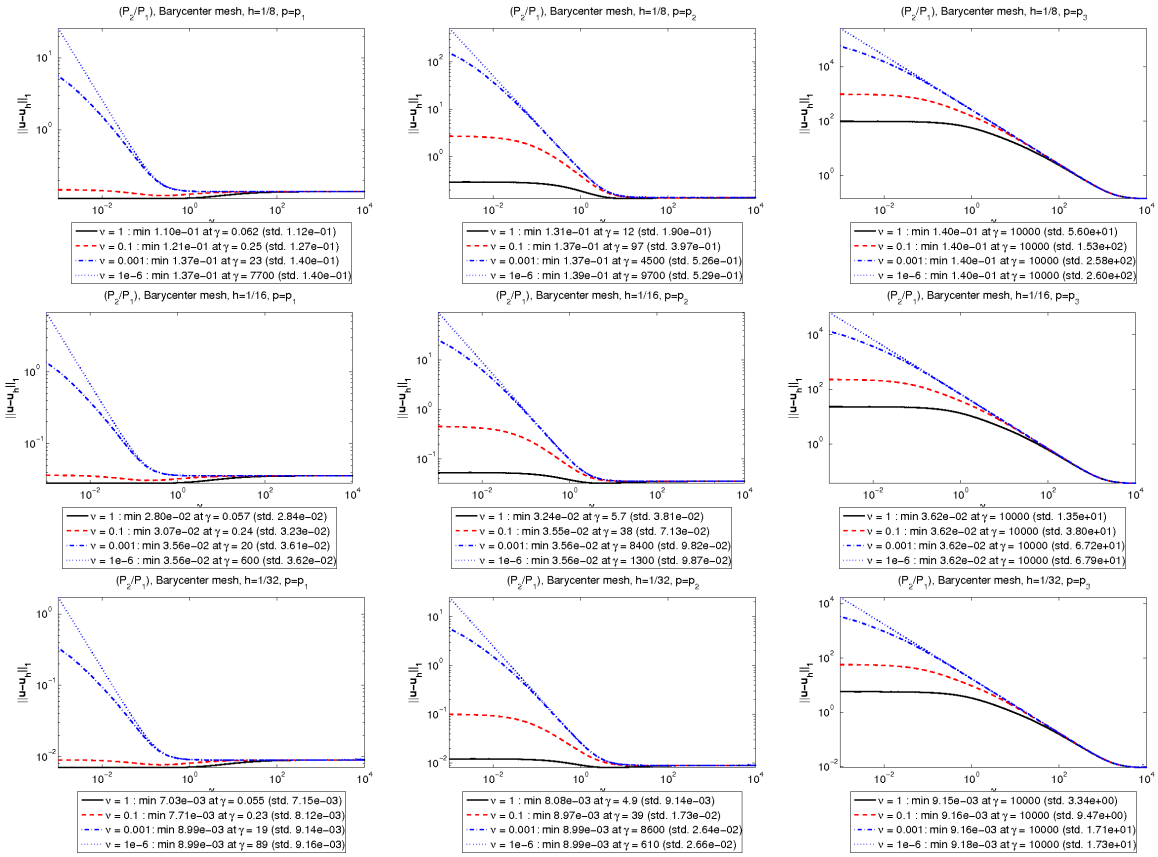

Fig. 2 $H^1(\Omega)$ velocity errors vs. grad-div stabilization parameter γ, for each of the Stokes solutions, on successive refinements of barycenter-refined uniform meshes, "std" gives the error for $\gamma = 1$.

the optimal parameter γ on ν, which is predicted in (3.10) together with $|\mathbf{u}|_3$ being independent of ν, can be observed as well.

Results for the $L^2(\Omega)$ pressure error are shown in Figure 3. We could observe that for all pressures and for all viscosities, the pressure error was almost constant and the relative change in the pressure error was very small for varying γ. For this reason, numerical errors, like round-off errors (in particular in the case of small viscosities), might have influence in the determination of the optimal parameter and we are not sure if it is possible to draw reliable conclusions with respect to all aspects of the prediction (3.18) on the basis of these results. Also, one should keep in mind that (3.18) was derived under the assumption of the maximal possible second term in (3.16). For the sake of brevity, only the results for p_3 are presented and discussed in some detail. Similar discussions could be performed for p_1 and p_2. First of all, it was predicted in Remark 2 that the optimal stabilization parameter for the pressure error is smaller than for the velocity error. This behavior can be seen clearly for all simulations. Then, we could observe that the optimal γ generally increases with increasing pressure norm $|p|_2$ and in Figure 3 one can see that the optimal γ does not depend on the mesh width. Both observation are conform with (3.18). However, in Figure 3, a dependence of the optimal γ on ν can be observed, which is not predicted by (3.18). The dependence is inverse to the velocity case. At the moment, one possible explanation are the round-off errors mentioned above.

4.1.2 $((P_2)^2, P_1)$ *Taylor–Hood element on Delaunay-generated triangulations*

Next, the case of $((P_2)^2, P_1)$ Taylor–Hood elements on a Delaunay-generated triangulation is considered, which is a situation where it is not expected that the pointwise divergence-free subspace of the velocity

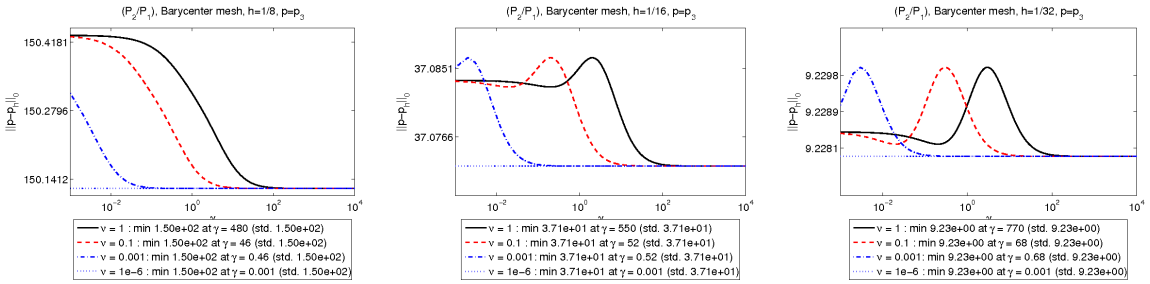

Fig. 3 $L^2(\Omega)$ pressure errors vs. grad-div stabilization parameter γ, for p_3 on three barycenter refined triangulations with $h \in \{1/8, 1/16, 1/32\}$, "std" gives the error for $\gamma = 1$.

space has optimal approximation properties. Hence, the parameter choice (3.7) should be applied, such that

$$\gamma_{\text{good}} \approx \begin{cases} \dfrac{C_0}{\sqrt{8\pi}} & \text{for } p_1, \\ \dfrac{C_0\sqrt{32}}{\pi} & \text{for } p_2, \\ \dfrac{C_0 10^4}{\sqrt{8\pi}} & \text{for } p_3. \end{cases} \tag{4.2}$$

The test problems were computed on three successively finer Delaunay-generated triangulations with $h \in \{1/8, 1/16, 1/32\}$. The mesh with $h = 1/16$ is depicted in Figure 1.

The results with respect to the error in the $H^1(\Omega)$ velocity norm are displayed in Figure 4. Again, the behavior of the numerical results in comparison with the analytical predictions will be discussed. From (4.2) one does not expect a dependence of the optimal stabilization parameter on the viscosity. This behavior can be observed rather well for p_1 and p_2 (first and second column), except for the case $\nu = 10^{-6}$. But note that in this case the error is almost constant in a wide range of γ and the round-off errors might have influence particularly in this case. Next, a moderate increase of the optimal γ between p_1 and p_2 is expected from (4.2). Comparing with the other case of a subspace with optimal approximation property, (4.1) and Figure 2, the increase should be smaller in the present case. Both predictions can be observed well in the numerical results. Further, very large optimal parameters are expected for large $|p|_2$, which is clearly seen for p_3 (third column). Finally, a dependence of the optimal parameter on the mesh width is not predicted from (4.2). Also this feature can be observed. The estimated mean value of C_0 from (4.2) was 6.45 and the median was 3.00.

From the prediction (4.2), one can expect that for each pressure there is a parameter choice, which is independent of the mesh width and the viscosity, that should give good results. In Figure 4 one can see that such choices are $\gamma = 1$ for p_1, $\gamma = 5$ for p_2, and $\gamma = 10^4$ for p_3. Since inserting (3.7) into the error estimate (3.5) leads to the dependence on $\nu^{-1/2}$ of terms on the right hand side of the estimate, see (3.8), one expects to see an increase of the error for the optimal stabilization parameter if ν decreases. For p_1 and p_2 (first and second column), this increase can be observed. One cannot see this effect for p_3. We think that again round-off errors are responsible. The case p_3 requires a very large γ, see (4.2), and then the grad-div contribution in the velocity-velocity coupling dominates the contribution from the viscous term. In the numerics, the round-off errors arising in adding terms of much different magnitudes annihilate the contribution of the viscous term.

With respect to the $L^2(\Omega)$ norm of the pressure, we could again observe that the error was almost constant in a wide range of γ. For this reason, we present again only the results obtained for p_3, see Figure 5. Most importantly, one can clearly see that the optimal γ is smaller than for the $H^1(\Omega)$ error of the velocity, as it was predicted in Remark 2. In addition, one can see that the optimal γ decreases with decreasing ν, which was also predicted. For p_3, one gets larger optimal γ with decreasing mesh width, although in (3.17) a mesh dependence does not occur. However, because of the very small relative changes of the pressure errors and the possible influence of round-off errors, in our opinion, the last two observations should not be used for conclusive statements.

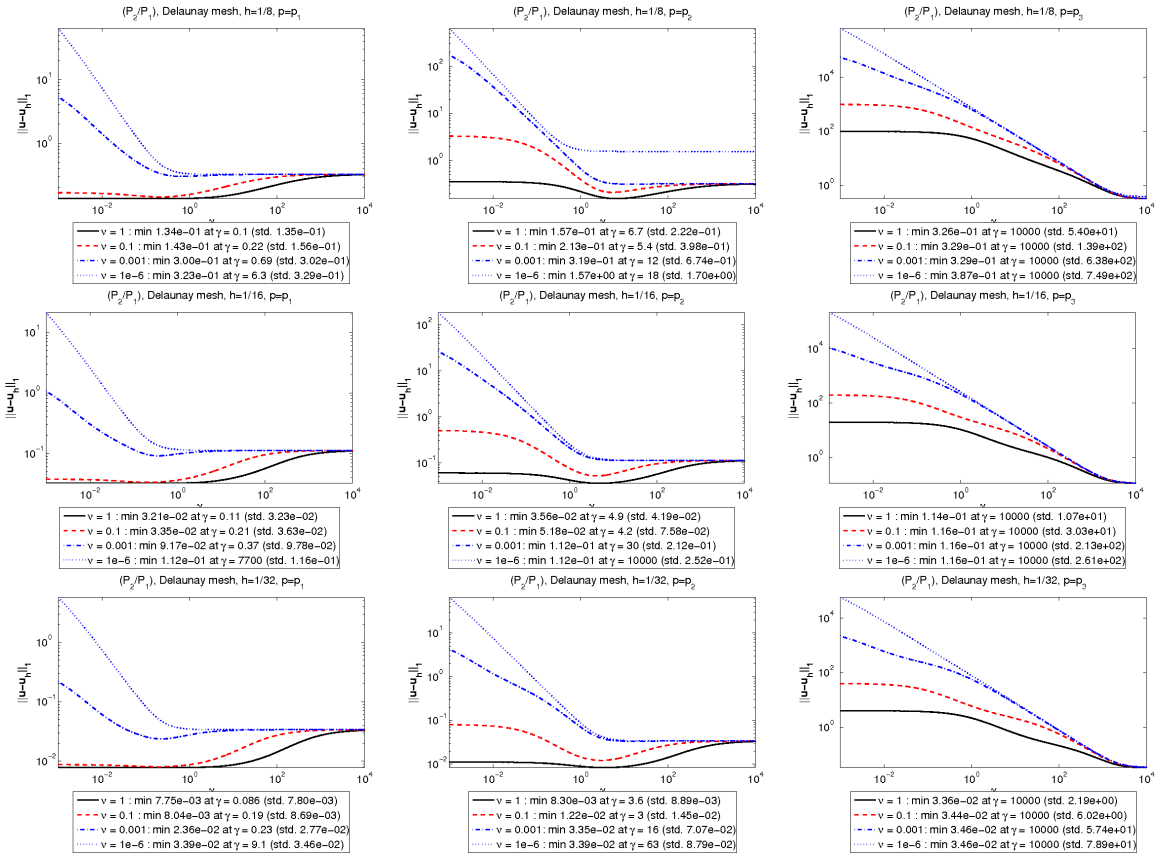

Fig. 4 $H^1(\Omega)$ velocity errors vs. grad-div stabilization parameter γ, for each of the Stokes solutions, on three Delaunay-generated triangulations with $h \in \{1/8, 1/16, 1/32\}$, "std" gives the error for $\gamma = 1$.

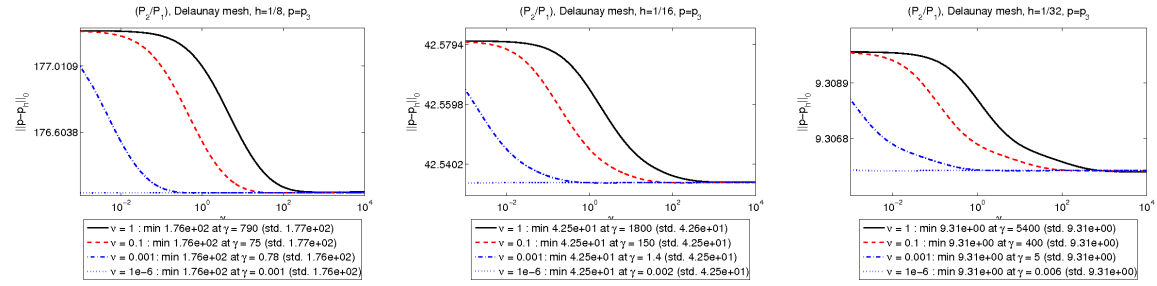

Fig. 5 $L^2(\Omega)$ pressure errors vs. grad-div stabilization parameter γ, for p_3 on three Delaunay-generated triangulations with $h \in \{1/8, 1/16, 1/32\}$, "std" gives the error for $\gamma = 1$.

4.1.3 The MINI element on Union Jack triangulations

Now, the MINI element $((P_1^{\text{bub}})^2, P_1)$ is considered, which was first studied in [1]. The simulations were performed on meshes of Union Jack type with $h \in \{1/16, 1/32, 1/64\}$, see the right hand side picture in Figure 1 for the coarsest of these meshes. From [33] it is known that on this type of meshes the MINI element has the property that the pointwise divergence-free subspace of the velocity space has optimal approximation properties. Arguing the same way as for the Taylor–Hood finite element, the theory derived

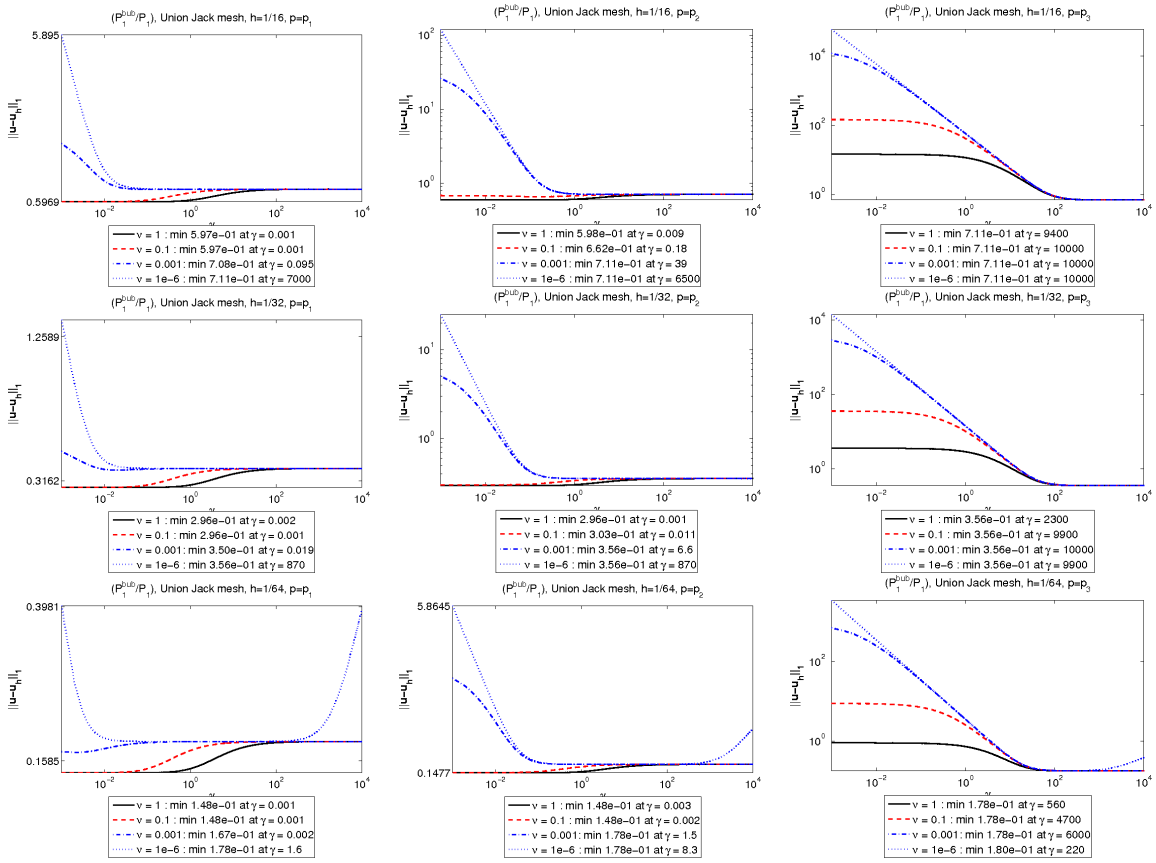

Fig. 6 $H^1(\Omega)$ velocity errors vs. grad-div stabilization parameter γ, for each of the Stokes solutions, using the MINI element on Union Jack triangulations with $h \in \{1/16, 1/32, 1/64\}$. We think that round-off errors influenced the simulations with the largest stabilization parameters and $\nu = 10^{-6}$ on the finest mesh.

in the previous section predicts that a good choice of γ should satisfy

$$\gamma_{\text{good}} \approx \frac{C_0 h^2}{2\nu} \frac{|p|_2^2}{|\mathbf{u}|_2^2} = \begin{cases} C_0 \dfrac{h^2}{4\nu} & \text{for } p_1, \\ 64 C_0 \dfrac{h^2}{\nu} & \text{for } p_2, \\ 2.5 \cdot 10^7 C_0 \dfrac{h^2}{\nu} & \text{for } p_3. \end{cases} \tag{4.3}$$

Note that there is now a dependence of the parameter on the mesh width, which comes from the equal-order interpolation of the velocity and pressure finite element space. Asymptotically, one has $\gamma_{\text{good}} = \mathcal{O}(h^2/\nu)$ and in particular $\gamma_{\text{good}} \to 0$ as $h \to 0$.

The results of the numerical simulations are presented in Figure 6. From (4.3), one predicts decreasing optimal stabilization parameters for decreasing mesh sizes. This expectation is always met. Similarly, the increase of the optimal stabilization parameter for small viscosities can be observed well for p_1 and p_2. For p_3, there is one exception concerning this issue, the computation for $\nu = 10^{-6}$ on the grid with $h = 1/64$. We think that round-off errors might gained some influence in the simulations with the largest stabilization parameters. For C_0 in (4.3), the mean value 0.068 and the median 0.075 was estimated.

For the same reason as discussed in Sect. 4.1.1, no dependence of the error for the optimal stabilization parameter on ν is expected. This expectation is met.

4.1.4 The MINI element on Delaunay-generated triangulations

Finally, the MINI element on Delaunay-generated triangulations will be considered, where one does not expect the divergence-free subspace of the velocity space to have optimal approximation properties. Hence,

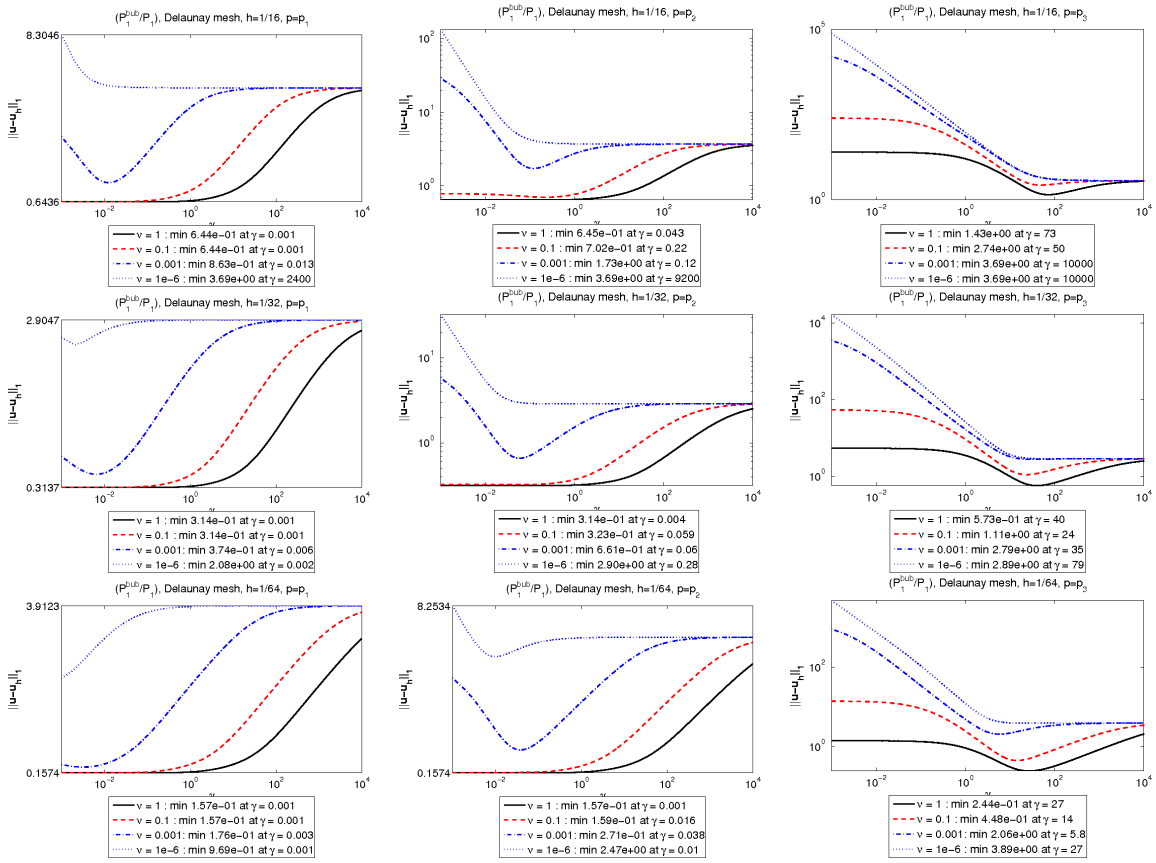

Fig. 7 $H^1(\Omega)$ velocity errors vs. grad-div stabilization parameter γ, for each of the Stokes solutions, using the MINI element on Delaunay-generated triangulations with $h \in \{1/16, 1/32, 1/64\}$.

the optimal stabilization parameter should be derived with the same arguments that were used to get (3.7), such that

$$\gamma_{\text{good}} \approx C_0 h \frac{|p|_2}{|\mathbf{u}|_2} = \begin{cases} \dfrac{C_0}{\sqrt{2}} h & \text{for } p_1, \\ 8\sqrt{2} C_0 h & \text{for } p_2, \\ 5000\sqrt{2} C_0 h & \text{for } p_3. \end{cases} \tag{4.4}$$

Figure 7 presents the results of the numerical simulations. In accordance with the expectations from (4.4), the optimal parameter decreases with mesh refinement. A dependence on the viscosity is not predicted. Save on the coarsest mesh, this prediction is fulfilled. In addition, note that particularly for small viscosities the error is almost constant on these meshes in a wide interval that includes the optimal stabilization parameter. The estimated mean value of C_0 from (4.4) was 0.19 and the median 0.17.

In this case, one expects from (3.8) a dependence of the error for the optimal γ on $\nu^{-1/2}$. In fact, an increase of the error for small ν can be observed in Figure 7.

4.1.5 Outlook to more complicated situations

For applying the results of the analysis, it is crucial to know whether or not a pointwise divergence-free subspace with optimal approximation properties exists. A first idea for answering this question for unknown situations is based on the fact that the existence of such a subspace depends only on the finite element space (grid and element choice) but not on the concrete problem. Given a triangulation, one can consider the Stokes equations with different viscosities and with a prescribed solution which does not depend on the viscosity. Performing simulations as presented in this section, one monitors the dependence of the optimal stabilization parameter and of the error in the $H^1(\Omega)$ norm of the velocity on the viscosity. If there is a pointwise divergence-free subspace with optimal approximation property, the optimal parameter should

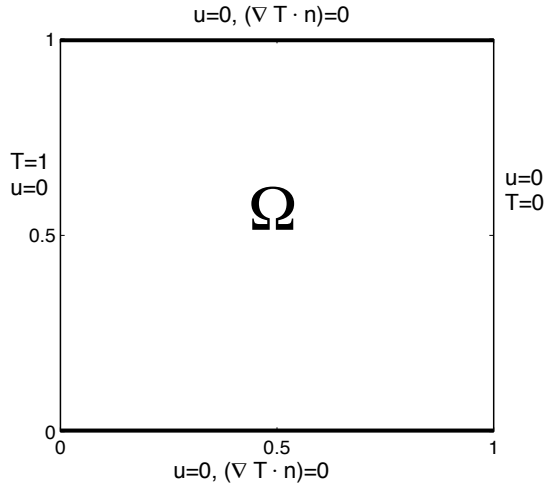

Fig. 8 The domain and boundary conditions for the natural convection problem.

increase for decreasing ν and the error should not depend on ν. For the other case, the situation should be vice versa. After having identified the case, an estimate for C_0 can be computed. The study of the practicability of this approach is outside the scope of this paper.

4.2 Rayleigh–Bénard convection for silicon oil

The second test problem we consider is the differentially heated cavity on the unit square with Rayleigh number $\mathrm{Ra} = 10^6$, Prandtl number $\mathrm{Pr} = \infty$ (corresponding to silicon oil), with no slip boundary conditions for the velocity, and mixed Dirichlet/Neumann conditions for the temperature, see Figure 8. Since $\mathrm{Pr} = \infty$, the system of equations that governs this flow is given by

$$\begin{aligned} -\Delta \mathbf{u} + \nabla p &= (0, \mathrm{Ra}\, T)^{\mathrm{T}} && \text{in } \Omega, \\ \nabla \cdot \mathbf{u} &= 0 && \text{in } \Omega, \\ -\Delta T + \mathbf{u} \cdot \nabla T &= 0 && \text{in } \Omega. \end{aligned}$$

Although this system is nonlinear because of the energy equation, the momentum equation is a Stokes equation. Thus, the theory developed in this paper is applicable.

This system was implemented with a standard finite element approach, see, e.g., [11], using $(V_h, Q_h) = ((P_2)^2, P_1)$ Taylor–Hood elements to approximate velocity and pressure, respectively, and $X_h = P_2$ to approximate temperature. The finite element formulation for a specified Ra takes the form: Find $(\mathbf{u}_h, p_h, T_h - T_{d,h}) \in V_h \times Q_h \times X_h$ such that for all $(\mathbf{v}_h, q_h, s_h) \in V_h \times Q_h \times X_h$

$$\begin{aligned} \nu(\nabla \mathbf{u}_h, \nabla \mathbf{v}_h) + \gamma(\nabla \cdot \mathbf{u}_h, \nabla \cdot \mathbf{v}_h) - (\nabla \cdot \mathbf{v}_h, p_h) &= ((0, \mathrm{Ra}\, T_h)^{\mathrm{T}}, \mathbf{v}_h), \\ (\nabla \cdot \mathbf{u}_h, q_h) &= 0, \\ (\nabla T_h, \nabla s_h) + (\mathbf{u} \cdot \nabla T_h, s_h) &= 0, \end{aligned} \tag{4.5}$$

where $T_{d,h}$ is an extension of the Dirichlet data to the finite element space with inhomogeneous Dirichlet boundary conditions. The nonlinearity of (4.5) is resolved using Newton's method, to a relative difference of 10^{-10} in successive iterates. We also found it necessary to use a continuation method in Ra to get convergence with $\mathrm{Ra} = 10^6$ (via $\mathrm{Ra} \in \{10^4, 10^5, 10^6\}$), and each Newton iteration typically took 4 or 5 iterations to converge. Plots of the resolved solution's velocity streamlines, pressure contours, speed contours, and temperature contours are shown in Figure 9. Observe that the size of the pressure p_h is on the order of 10^5, while the speed $|\mathbf{u}_h|^2$ is on the order of 10^2, and hence the size of the velocity is on the order 10^1. Thus, the ratio of the size of the pressure to the size of the velocity is very large, and from the contour plots one can expect $|p|_2/|\mathbf{u}|_3$ to be large as well. Considering this problem on a coarse mesh, a larger velocity error (compared with the reference solution) can be expected that is dominated by the contribution from the pressure. The analysis presented in this paper suggests that this contribution can be

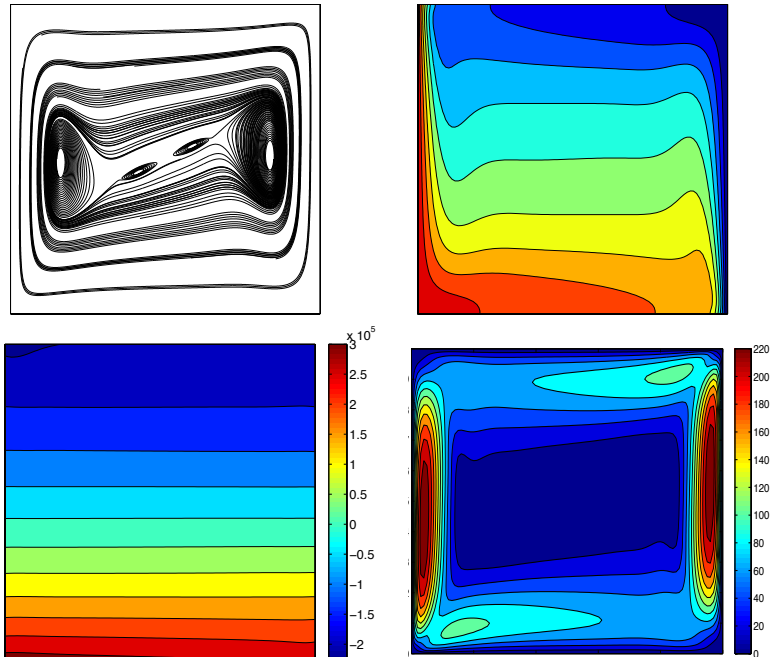

Fig. 9 The velocity streamlines (top left), temperature contours (top right), pressure contours (bottom left), and speed contours (bottom right) of the resolved solution to the differentially heated cavity.

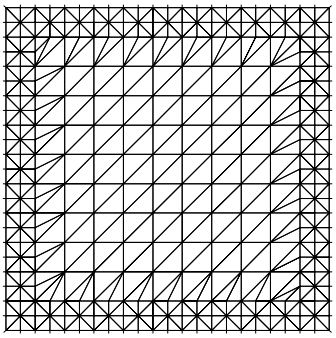

Fig. 10 The mesh used for the differentially heated cavity problem.

reduced by increasing the grad-div stabilization parameter γ, thereby reducing the overall error, and finally leading to significantly improved solutions for the velocity.

We computed solutions to (4.5), using $((P_2)^2, P_1, P_2)$ elements for velocity-pressure-temperature, on the mesh shown in Figure 10 that provided 3,679 total degrees of freedom, with varying grad-div stabilization parameter γ. Solutions are shown in Figure 11, as velocity streamlines and temperature contours. Comparing with the resolved solution in Figure 9, the temperature contours agree for all solutions except when $\gamma = 0$, but the velocity streamlines are correct only for the $\gamma = 1,000$ and $\gamma = 10,000$ simulations. Hence, one observes an increase in accuracy from the use of large grad-div stabilization parameters, as expected. A similar observation was reported in [7] for the case $\mathrm{Pr} = 1$.

5 Conclusions and outlook

A re-investigation of the question of optimal grad-div stabilization parameters in finite element methods for the Stokes equations was presented that clarified that one has to distinguish several situations for designing such a parameter for conforming inf-sup stable pairs of finite element spaces, depending on whether the $H^1(\Omega)$ error of the velocity or the $L^2(\Omega)$ error of the pressure is of interest. It was verified that the question of the existence of a divergence-free subspace with optimal approximation properties is crucial.

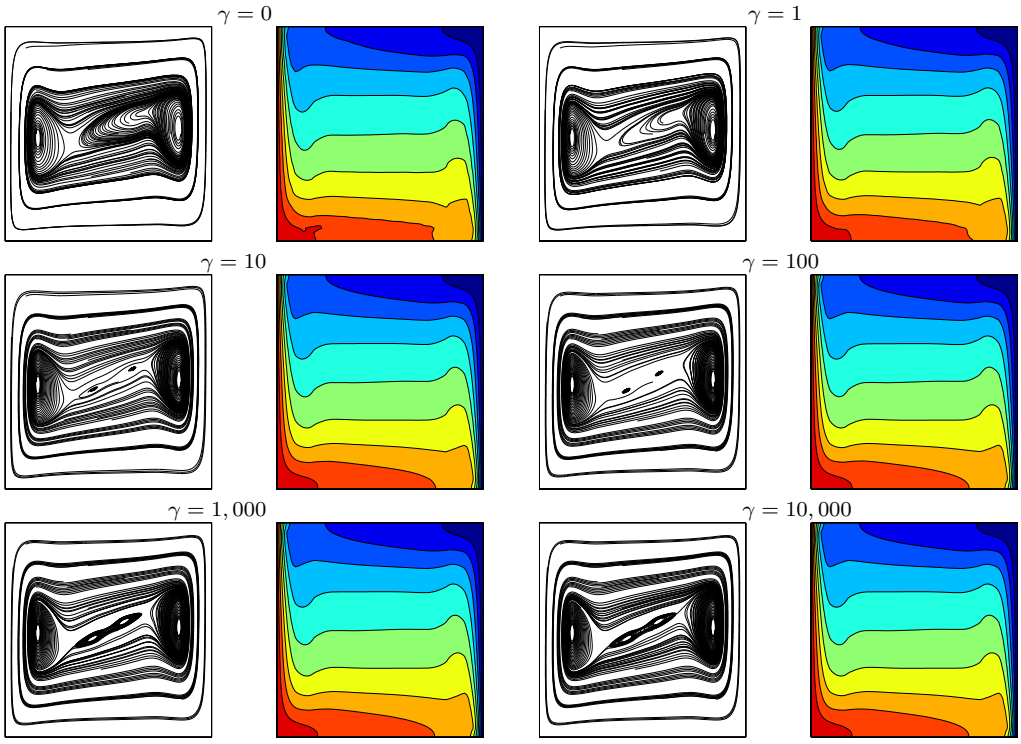

Fig. 11 Differentially heated cavity problem: velocity streamlines and temperature contours of solutions with varying γ.

Consequently, the optimal parameter choice does not even have the same expression within classes of finite element spaces, e.g., within the class of Taylor–Hood finite elements, as it depends on the concrete space itself, i.e., on the properties of the grid and the element choice together. In addition, the regularity of the solution also plays a role for the optimal stabilization parameter. Based on estimate (3.1), one can derive parameters for solutions with reduced smoothness by applying interpolation estimates to spaces with appropriate regularity.

A main observation is that the bound of the error estimate for the $H^1(\Omega)$ error of the velocity does not depend directly on the viscosity and the pressure if a pointwise divergence-free subspace with optimal approximation properties exists and an appropriate stabilization parameter is used. It was shown that a good choice of the stabilization parameter for minimizing the $H^1(\Omega)$ velocity error gives in many cases larger parameters than obtained for minimizing the $L^2(\Omega)$ error of the pressure. For the MINI element, good stabilization parameters were derived on the basis of the present analysis which seem to be new.

The present paper gave an analytic support for the observation from [11] that the use of large stabilization parameters is appropriate in certain situations. Numerical studies were presented that support the analytic results. Moreover, and particularly important for applications, an enormous error reduction (in the $H^1(\Omega)$ error of the velocity) could be observed in certain cases by using parameters predicted on the basis of the present analysis instead of parameters of $\mathcal{O}(1)$, as they were proposed in the literature (based on error estimates for other norms). Also in a more complex flow problem, the choice of large stabilization parameters resulted in considerable improvements of the computed velocity field.

Extending the analytic considerations to more complex equations or systems from Computational Fluid Dynamics will result in more terms on the right hand side of the error estimates. Hence, it will become more complicated to derive information about a good value of the stabilization parameters. This issue will be studied in future work. Also from the practical point of view, a number of issues need to be addressed. How to determine whether the divergence-free subspace of the finite element velocity has optimal approximation properties? A first idea for answering this question was presented in Section 4.1.5. Or, how to estimate parameters of form (3.7) or (3.9) efficiently without knowledge of the analytic solution? Altogether, there are a number of topics for further research on the grad-div stabilization.

Acknowledgment. We would like to acknowledge two unknown referees whose valuable hints helped to improve this paper considerably.

References

1. D. Arnold, F. Brezzi, and M. Fortin. A stable finite element for the Stokes equations. Calcolo, 21(4):337–344, 1984.
2. D. Arnold and J. Qin. Quadratic velocity/linear pressure Stokes elements. In R. Vichnevetsky, D. Knight, and G. Richter, editors, Advances in Computer Methods for Partial Differential Equations VII, pages 28–34. IMACS, 1992.
3. M. Braack, E. Burman, V. John, and G. Lube. Stabilized finite element methods for the generalized Oseen problem. Comput. Methods Appl. Mech. Engrg., 196(4-6):853–866, 2007.
4. S. Brenner and L. R. Scott. The Mathematical Theory of Finite Element Methods. Springer-Verlag, 1994.
5. Y. Bychenkov and E.V. Chizonkov. Optimization of one three-parameter method of solving an algebraic system of Stokes type. Russ. J. Numer. Anal. Math. Model, 14:429–440, 1999.
6. M. Case, V. Ervin, A. Linke, and L. Rebholz. A connection between Scott-Vogelius elements and grad-div stabilization. SIAM Journal on Numerical Analysis, 49(4):1461–1481, 2011.
7. O. Dorok, W. Grambow, and L. Tobiska. Aspects of finite element discretizations for solving the Boussinesq approximation of the Navier-Stokes Equations. Notes on Numerical Fluid Mechanics: Numerical Methods for the Navier-Stokes Equations. Proceedings of the International Workshop held at Heidelberg, October 1993, ed. by F.-K. Hebeker, R. Rannacher and G. Wittum, 47:50–61, 1994.
8. L. Franca and T. Hughes. Two classes of mixed finite element methods. Computer Methods in Applied Mechanics and Engineering, 69(1):89–129, 1988.
9. Leopoldo P. Franca and Saulo P. Oliveira. Pressure bubbles stabilization features in the Stokes problem. Comput. Methods Appl. Mech. Engrg., 192(16-18):1929–1937, 2003.
10. freeFEM.org. freeFEM. `http://www.freefem.org/`.
11. K. Galvin, A. Linke, L. Rebholz, and N. Wilson. Stabilizing poor mass conservation in incompressible flow problems with large irrotational forcing and application to thermal convection. Computer Methods in Applied Mechanics and Engineering, 237:166–176, 2012.
12. T. Gelhard, G. Lube, M. Olshanskii, and J. Starcke. Stabilized finite element schemes with LBB-stable elements for incompressible flows. J. Comput. Math., 177:243–267, 2005.
13. R. Glowinski and P. Le Tallec. Augmented Lagrangian and operator splitting methods in nonlinear mechanics. SIAM, Studies in Applied Mathematics, Philadelphia, 1989.
14. T. Heister and G. Rapin. Efficient augmented Lagrangian-type preconditioner for the Oseen problem using grad-div stabilization. Int. J. Numer. Meth. Fluids, 71:118–134, 2013.
15. V. John and A. Kindl. Numerical studies of finite element variational multiscale methods for turbulent flow simulations. Comput. Methods Appl. Mech. Engrg., 199(13-16):841–852, 2010.
16. V. John and G. Matthies. MooNMD - a program package based on mapped finite element methods. Comput. Vis. Sci., 6(2–3):163–170, 2004.
17. W. Layton. An Introduction to the Numerical Analysis of Viscous Incompressible Flows. SIAM, 2008.
18. W. Layton, C. Manica, M. Neda, M. A. Olshanskii, and L. Rebholz. On the accuracy of the rotation form in simulations of the Navier-Stokes equations. Journal of Computational Physics, 228(9):3433–3447, 2009.
19. A. Linke, L. Rebholz, and N. Wilson. On the convergence rate of grad-div stabilized Taylor-Hood to Scott-Vogelius solutions for incompressible flow problems. Journal of Mathematical Analysis and Applications, 381:612–626, 2011.
20. G. Lube and M. Olshanskii. Stable finite element calculations of incompressible flows using the rotation form of convection. IMA J.Num.Anal., 22:437–461, 2002.
21. Gert Lube and Gerd Rapin. Residual-based stabilized higher-order FEM for a generalized Oseen problem. Math. Models Methods Appl. Sci., 16(7):949–966, 2006.
22. C. Manica, M. Neda, M. A. Olshanskii, and L. Rebholz. Enabling accuracy of Navier-Stokes-alpha through deconvolution and enhanced stability. M2AN: Mathematical Modelling and Numerical Analysis, 45:277–308, 2011.
23. M. A. Olshanskii. A low order Galerkin finite element method for the Navier-Stokes equations of steady incompressible flow: a stabilization issue and iterative methods. Comput. Meth. Appl. Mech. Eng., 191:55155536, 2002.
24. M. A. Olshanskii, G. Lube, T. Heister, and J. Löwe. Grad-div stabilization and subgrid pressure models for the incompressible Navier-Stokes equations. Comput. Methods Appl. Mech. Engrg., 198(49-52):3975–3988, 2009.
25. M. A. Olshanskii and A. Reusken. Grad-Div stabilization for the Stokes equations. Math. Comp., 73:1699–1718, 2004.
26. Roger Pierre. Simple C^0 approximations for the computation of incompressible flows. Comput. Methods Appl. Mech. Engrg., 68(2):205–227, 1988.
27. J. Qin. On the convergence of some low order mixed finite elements for incompressible fluids. PhD thesis, Pennsylvania State University, 1994.
28. H.-G. Roos, M. Stynes, and L. Tobiska. Numerical methods for singularly perturbed differential equations, volume 24 of Springer Series in Computational Mathematics. Springer-Verlag, Berlin, 1996. Convection-diffusion and flow problems.
29. H.-G. Roos, M. Stynes, and L. Tobiska. Robust numerical methods for singularly perturbed differential equations, volume 24 of Springer Series in Computational Mathematics. Springer, Berlin, 2nd edition, 2008.
30. L. Tobiska and R. Verfürth. Analysis of a streamline diffusion finite element method for the Stokes and Navier-Stokes equations. SIAM J. Numer. Anal., 33:107–127, 1996.
31. S. Zhang. A new family of stable mixed finite elements for the 3d Stokes equations. Math. Comp., 74(250):543–554, 2005.
32. S. Zhang. On the P1 Powell-Sabin divergence-free finite element for the Stokes equations. J. Comput. Math., 26(3):456–470, 2008.
33. S. Zhang. Bases for C0-P1 divergence-free elements and for C1-P2 finite elements on union jack grids. Submitted, 2012.